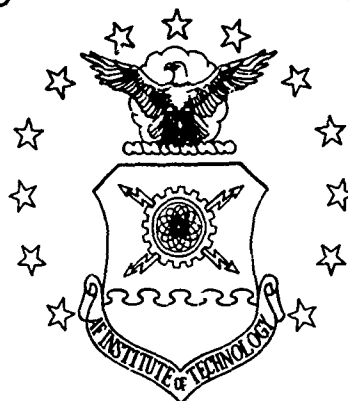
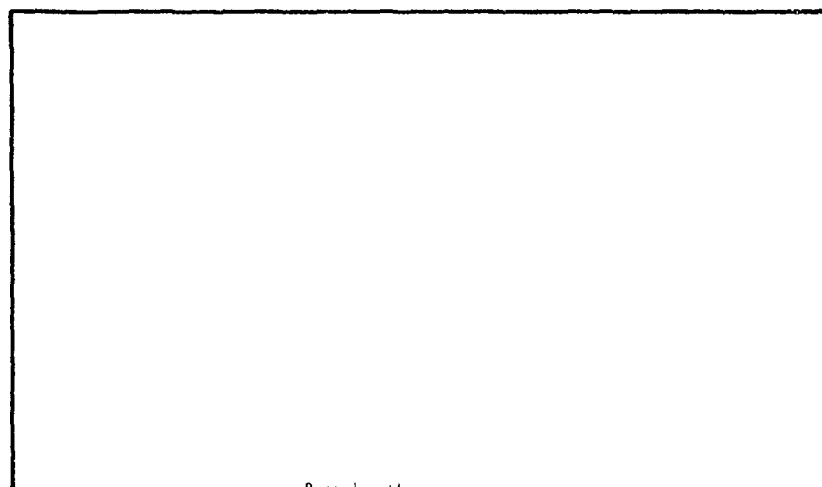


AD753387

**AIR FORCE INSTITUTE OF TECHNOLOGY**



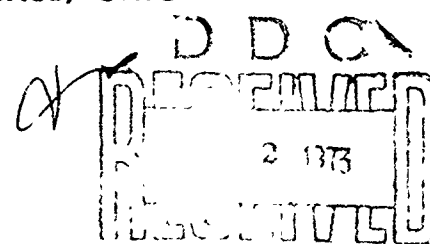
**AIR UNIVERSITY  
UNITED STATES AIR FORCE**



Reproduced by  
**NATIONAL TECHNICAL  
INFORMATION SERVICE**  
U.S. Department of Commerce  
Springfield, VA 22151

**SCHOOL OF ENGINEERING**

**WRIGHT-PATTERSON AIR FORCE BASE, OHIO**



Unclassified

Security Classification

## DOCUMENT CONTROL DATA - R &amp; D

(Security classification of title, body of abstract and indexing annotation must be entered when the overall report is classified)

1. ORIGINATING ACTIVITY (Corporate author) <b>Air Force Institute of Technology Wright-Patterson Air Force Base, Ohio 45433</b>		2a. REPORT SECURITY CLASSIFICATION <b>Unclassified</b>	
		2b. GROUP	
3. REPORT TITLE <b>AN ANALYSIS OF THE FLOW FIELD AROUND A 2-D BODY OF ARBITRARY SHAPE</b>			
4. DESCRIPTIVE NOTES (Type of report and inclusive dates) <b>AFIT Thesis</b>			
5. AUTHOR(S) (First name, middle initial, last name) <b>Ellie B. Underwood, Jr. Capt USAF</b>			
6. REPORT DATE <b>December 1971</b>		7a. TOTAL NO. OF PAGES <b>27 87</b>	7b. NO. OF REFS <b>4</b>
8a. CONTRACT OR GRANT NO.		9a. ORIGINATOR'S REPORT NUMBER(S) <b>GAM-AE/72-2</b>	
b. PROJECT NO. <b>N/A</b>			
c.		9b. OTHER REPORT NO(S) (Any other numbers that may be assigned this report)	
d.			
10. DISTRIBUTION STATEMENT <b>Approved for public release; distribution unlimited.</b>			
Approved for public release; IAW AFR 190-17 <b>JERRY C. HIX, Captain, USAF Director of Information</b>		11. SPONSORING MILITARY ACTIVITY <b>AFIT-EN</b>	
13. ABSTRACT <b>An analytical study of the two-dimensional viscous, incompressible steady flow over an airfoil of arbitrary shape was made. Theodorsen's method was used to analyze the potential flow around the airfoil, providing edge velocities for the boundary layer equations, which were then solved by the Karman-Pohlhausen method. The resulting boundary layer displacement thickness was then added to the original airfoil shape to obtain a better potential flow solution. Iteration was continued in this manner until the desired accuracy was obtained. A computer program was written to effect this airfoil analysis technique. Potential flow surface velocity distribution, angle of attack at zero lift, and wall shearing stress were shown to agree well with results of other investigators.</b>			

-1a-

DD FORM 1473

Unclassified

14.

KEY WORDS

Airfoil

Theodorsen

Conformal transformation

Potential flow

Boundary layer

LINK A

LINK B

LINK C

ROLE

WT

ROLE

WT

ROLE

WT

AN ANALYSIS OF THE FLOW FIELD AROUND A 2-D  
BODY OF ARBITRARY SHAPE

THESIS

Presented to the Faculty of the School of Engineering  
of the Air Force Institute of Technology  
Air University  
in Partial Fulfillment of the  
Requirements for the Degree of  
Master of Science

by

Ellie B. Underwood, Jr., B.S.A.S.E.  
Captain USAF  
Graduate Aeronautical Engineering

December 1971

-ic-

Approved for public release; distribution unlimited.

Contents

List of Figures . . . . .	iii
List of Tables . . . . .	iv
List of Symbols . . . . .	v
Abstract . . . . .	viii
I. Introduction . . . . .	1
II. Theodorsen's Method . . . . .	6
III. Karman-Pohlhausen Method . . . . .	21
IV. Computer Study . . . . .	33
V. Results . . . . .	36
VI. Conclusions and Recommendations . . . . .	43
Bibliography . . . . .	45
Appendix A: Computer Program and Sample Output Format . . . . .	46
Vita . . . . .	

List of Figures

<u>Figure</u>		<u>Page</u>
1	Transformation Planes and Notation . . . .	10
2	Boundary Layer Coordinate System . . . . .	22
3	Transformation of NACA 4424 Airfoil . . .	38
4	Pressure Distribution on NACA 1408 Airfoil	39
5	Shear Stress on NACA 1408 Airfoil . . . .	40
6	Boundary Layer Displacement Thickness on NACA 1408 Airfoil . . . . .	41

List of Tables

<u>Table</u>		<u>Page</u>
1	Comparison of Zero Lift Angles of Attack . . . . .	36
2	Comparison of Potential Flow Velocities for NACA 1408 Airfoil . . . . .	37

List of SymbolsFor Theodorsen's Method

<u>Symbol</u>	<u>Description</u>
$a$	Dimensional proportionality constant (length)
$A_n, B_n, C_n$	Fourier coefficients
$i$	$\sqrt{-1}$
$m$	Intermediate quantity in Joukowski transformation, defined on page 9
$R$	Radius vector in exact circle plane
$u$	Velocity in x-direction
$V$	Potential flow surface velocity
$V_\infty$	Freestream velocity
$v$	Velocity in y-direction
$w$	Complex potential function
$x$	Cartesian coordinate in freestream flow direction
$y$	Cartesian coordinate perpendicular to free-stream flow direction
$z$	Complex position vector in exact circle plane
$z'$	Complex position vector in pseudo-circle plane
$\alpha$	Angle of attack
$\beta$	Angle of attack at zero lift
$\Gamma$	Circulation
$\epsilon$	Conformal angular distortion function
$\zeta$	Complex position vector in airfoil plane
$\theta$	Angular measure in exact circle plane
$\lambda$	Dummy variable of integration corresponding to $\theta$



<u>Symbol</u>	<u>Description</u>
$\rho$	Radius vector in pseudo-circle plane
$\phi$	Potential function
$\phi$	Magnification exponent in exact circle plane
$\Psi$	Stream function
$\psi$	Magnification exponent in pseudo-circle plane, as a function of $\omega$
$\bar{\psi}$	$\psi$ , as a function of $\theta$
$\omega$	Angular measure in pseudo-circle plane

For Karman-Pohlhausen Method

<u>Symbol</u>	<u>Description</u>
$a, b, c, d$	Coefficients in assumed velocity profile
$F, f_1, f_2, Z, K$	Boundary layer parameters
$U$	Boundary layer edge velocity
$x$	Streamwise coordinate
$y$	Cross-stream coordinate
$\delta$	Boundary layer thickness
$\delta_1$	Boundary layer displacement thickness
$\delta_2$	Boundary layer momentum thickness
$\eta$	Cross-stream coordinate referenced to boundary layer thickness, $y/\delta$
$\Lambda$	Shape factor
$\mu$	Absolute viscosity
$\nu$	Dynamic viscosity
$\rho$	Fluid density
$\tau_w$	Shear stress at airfoil surface
$o$	Subscript indicating stagnation point

<u>Symbol</u>	<u>Description</u>
1	Subscript indicating first point downstream of stagnation point
n	Subscript indicating general point

## AN ANALYSIS OF THE FLOW FIELD AROUND A 2-D BODY OF ARBITRARY SHAPE

### I. Introduction

#### Purpose

The purpose of this study was to determine the velocity field and, therefore, the pressure distribution about a body of arbitrary shape in a two-dimensional, steady, incompressible, constant viscosity flow, utilizing a combination of Theodorsen's method and the Karman-Pohlhausen method. A computer program to implement this combined method has been written, and results from this program are described herein.

Some practical and theoretical considerations leading to this combined method are presented in the remainder of this section.

#### Background

The theoretical analysis or design of an airfoil shape is based primarily upon a knowledge of the velocity field in the neighborhood of the body. Since the time of Prandtl, aerodynamicists have realized that the flow over a body could be divided, for purposes of analysis, into two regions. Observations indicate that viscous forces predominate over inertia forces in a very thin layer near the surface of the body, and this region has come to be called the boundary layer. Outside this region, the flow may, with little error, be considered inviscid. Since inviscid flow with a

uniform parallel onset velocity may be described in terms of a velocity potential, the inviscid region is also called the region of potential flow. If the velocity field can be determined in the inviscid flow, then the velocity at the edge of the boundary layer will be known and may be used as a boundary condition for solution of the boundary layer equations. Each of these regions will now be considered.

#### Region of Inviscid Flow

For thin streamlined airfoils at low angles of attack, small perturbation theory permits a number of simplifying assumptions in the equations of motion for inviscid flow. However, no such simplified potential theory was available for airfoils of arbitrary shape until 1933, when Theodorsen's method (Ref 2) was published.

Theodorsen made use of the fact that any closed curve, such as an airfoil, defined in the complex plane, may be transformed mathematically into a circle. This transformation may be further required to be conformal; that is, to preserve the local angular relationship between lines passing through each point. Conformality, therefore, ensures that the angle of attack of the airflow is unaffected by the transformation. The problem then becomes that of analyzing the two-dimensional flow over a circle. Since this is one of the very few cases for which exact solutions to the equations of motion are known, the velocity at each point

on the circle may be obtained immediately. Then, through an inverse transformation, the potential flow velocity at the corresponding point on the surface of the airfoil may also be determined. This velocity may be used as an approximation, (since boundary layer thickness has not yet been accounted for) to the velocity at the edge of the boundary layer.

Straightforward though this method appears, its use before the advent of high-speed computers was limited in practice by the enormity of the task of solving the necessary integral equations iteratively to the desired accuracy. The transformation is very time-consuming and tedious when performed by hand, providing numerous opportunities to make minor mathematical errors which may invalidate subsequent work. Since these are precisely the disadvantages in computation that a digital computer is designed to overcome, Theodorsen's method lends itself well to formulation for machine use.

The rate at which the iterative solution converges is largely dependent upon how nearly the original airfoil approximates a circle. Therefore, Theodorsen recommends the use of an intermediate analytical transformation (the Joukowski transformation) which converts the airfoil shape into a pseudo-circle conformally, and, thereby, reduces the computation time required.

Boundary Layer Region

The boundary layer equations may be derived from the Navier-Stokes equations for viscous fluid motion under the assumptions of steady, incompressible, constant viscosity flow at large Reynold's numbers. The Karman-Pohlhausen method (Ref 3) of solving the boundary layer equations is based on the further assumption that the velocity profile may be adequately represented as a fourth-degree polynomial satisfying appropriate boundary conditions, including the edge velocity distribution previously found from Theodorsen's method.

Combined Flow Fields

The boundary layer flow determined from the Karman-Pohlhausen method is only a first approximation, because a body with a boundary layer appears to the potential flow to be thicker by the amount of the displacement thickness. Therefore, the displacement thickness of the boundary layer must be computed for the approximate edge velocity; then this thickness must be added to the actual thickness of the body; and the inviscid velocity field for the resulting shape determined by Theodorsen's method. Thus, the velocity field solutions are continually refined until the change in displacement thickness from one iteration to the next is negligible. At this point, the problem of finding the velocity field may be considered solved. With the velocity field known, other aerodynamic parameters such as lift,

drag, circulation, and separation point may also be computed, using standard methods.

## II. Theodorsen's Method

### Method of Presentation

Theodorsen's method of irrotational flow analysis depends upon several important results of potential theory and the theory of conformal transformations of complex functions. These results will be briefly summarized before a detailed presentation of the Joukowski and Theodorsen transformations is given. Finally, the process for obtaining surface velocities by an inverse transformation will be presented.

### Review of Potential Theory

The flow outside the boundary layer is assumed to be steady, irrotational, and incompressible, permitting its description in terms of a velocity potential  $\phi$  or a stream function  $\psi$ , defined so that:

$$\begin{aligned} u &= \frac{\partial \phi}{\partial x} = \frac{\partial \psi}{\partial y} && \text{velocity in x-direction} \\ v &= \frac{\partial \phi}{\partial y} = - \frac{\partial \psi}{\partial x} && \text{velocity in y-direction} \end{aligned} \tag{1}$$

The lines of constant  $\psi$  (streamlines) and lines of constant  $\phi$  (equipotential lines) are orthogonal families of curves.

Any functions of  $\phi$  and  $\psi$  which satisfy Laplace's equation,  $\nabla^2 \phi = \nabla^2 \psi = 0$ , represent possible types of fluid motion. The boundary conditions of impermeability of the airfoil surface and uniform flow at infinity define a unique solution.



Conformal Transformation

If  $w(\zeta) = \phi(x,y) + i\psi(x,y)$  is an analytic function of the complex variable  $\zeta = x + iy$ , and the components  $\phi$  and  $\psi$  satisfy Laplace's equation, then certain useful relations exist between the  $\zeta$ -plane and the  $w$ -plane. Specifically, any simple curve  $f(\zeta)$ , such as an airfoil surface, maps into a curve  $f(w)$  in the  $w$ -plane in such a manner that the angles between pairs of lines passing through any point in the  $\zeta$ -plane remain unchanged at the image point in the  $w$ -plane, although local rotations and magnifications may occur. Therefore, the streamlines and equipotential lines of the  $\zeta$ -plane remain orthogonal in the plane of transformation. An exception occurs at points where  $\frac{dw}{d\zeta} = 0$ . These points correspond to flow stagnation points in the exact circle plane, and also in the airfoil plane, unless the trailing edge is cusped, in which case the airfoil has no trailing edge stagnation point.

Riemann has shown that the transformed curve may be specified without negating the conformal characteristic of the transformation. In particular, the interior of any simply-connected region can be mapped inside a circle, with the curve enclosing the region mapping onto the circumference of the circle. This transformation is unique when the origins and orientations of the coordinate systems in the two planes are specified.

Joukowski Transformation

The transformation  $\zeta = z' + a^2/z'$ , where the  $\zeta$ -plane is the plane of the airfoil ( $\zeta = x + iy$ ) is the Joukowski transformation. If the airfoil is elliptical or one of the special class of airfoils known as Joukowski airfoils, then a circle results in the  $z'$ -plane. If not, then a curve (pseudo-circle in Fig. 1) closely approximating a circle results for conventional airfoil shapes. While this transformation is not essential to Theodorsen's method, it improves the rate of convergence of the subsequent transformation. The constant "a" is included to preserve dimensions and has the dimension of length. The curve in the  $z'$ -plane can also be represented as  $z' = ae^{\psi+i\omega}$  in polar coordinates, where  $\rho = ae^{\psi}$  is the radius vector and the angular coordinate is  $\omega$ . Substituting the polar form of  $z'$  into the transformation equation yields

$$\zeta = 2a \cosh (\psi + i\omega) \quad (2)$$

or

$$\zeta = 2a \cosh \psi \cos \omega + 2ia \sinh \psi \sin \omega \quad (3)$$

Noting that  $\zeta = x + iy$ , and equating real and imaginary parts, the airfoil coordinates may be found explicitly in terms of the transformation coordinates

$$x = 2a \cosh \psi \cos \omega$$

$$y = 2a \sinh \psi \sin \omega \quad (4)$$

The inverse relations between coordinates will now be determined. Solving Eqs (4) for  $\cosh \psi$  and  $\sinh \psi$  and substituting into the identity  $\cosh^2 \psi - \sinh^2 \psi = 1$  gives

$$\left(\frac{x}{2a \cos \omega}\right)^2 - \left(\frac{y}{2a \sin \omega}\right)^2 = 1 \quad (5)$$

which can be solved for  $\omega$

$$\omega = \sin^{-1} \sqrt{1/2 \{n + \sqrt{n^2 + (y/a)^2}\}} \quad (6)$$

where

$$n = 1 - \left(\frac{x^2 + y^2}{4a^2}\right)$$

Likewise, Eqs (4) may be solved for  $\cos \omega$  and  $\sin \omega$  and substituted into the identity  $\cos^2 \omega + \sin^2 \omega = 1$ , giving

$$\left(\frac{x}{2a \cosh \psi}\right)^2 + \left(\frac{y}{2a \sinh \psi}\right)^2 = 1 \quad (7)$$

so that,

$$\psi = \sinh^{-1} \sqrt{1/2 \{-n + \sqrt{n^2 + (y/a)^2}\}} \quad (8)$$

#### Theodorsen Transformation

$$\sum_{n=0}^{\infty} \frac{C_n}{z^n}$$

The Theodorsen transformation  $z' = z e$  maps the pseudo-circle in the  $z'$ -plane into an exact circle (Fig. 1) in the  $z$ -plane. The coefficients  $C_n$  are complex numbers of the form  $A_n + iB_n$ . The condition that the flow at infinity

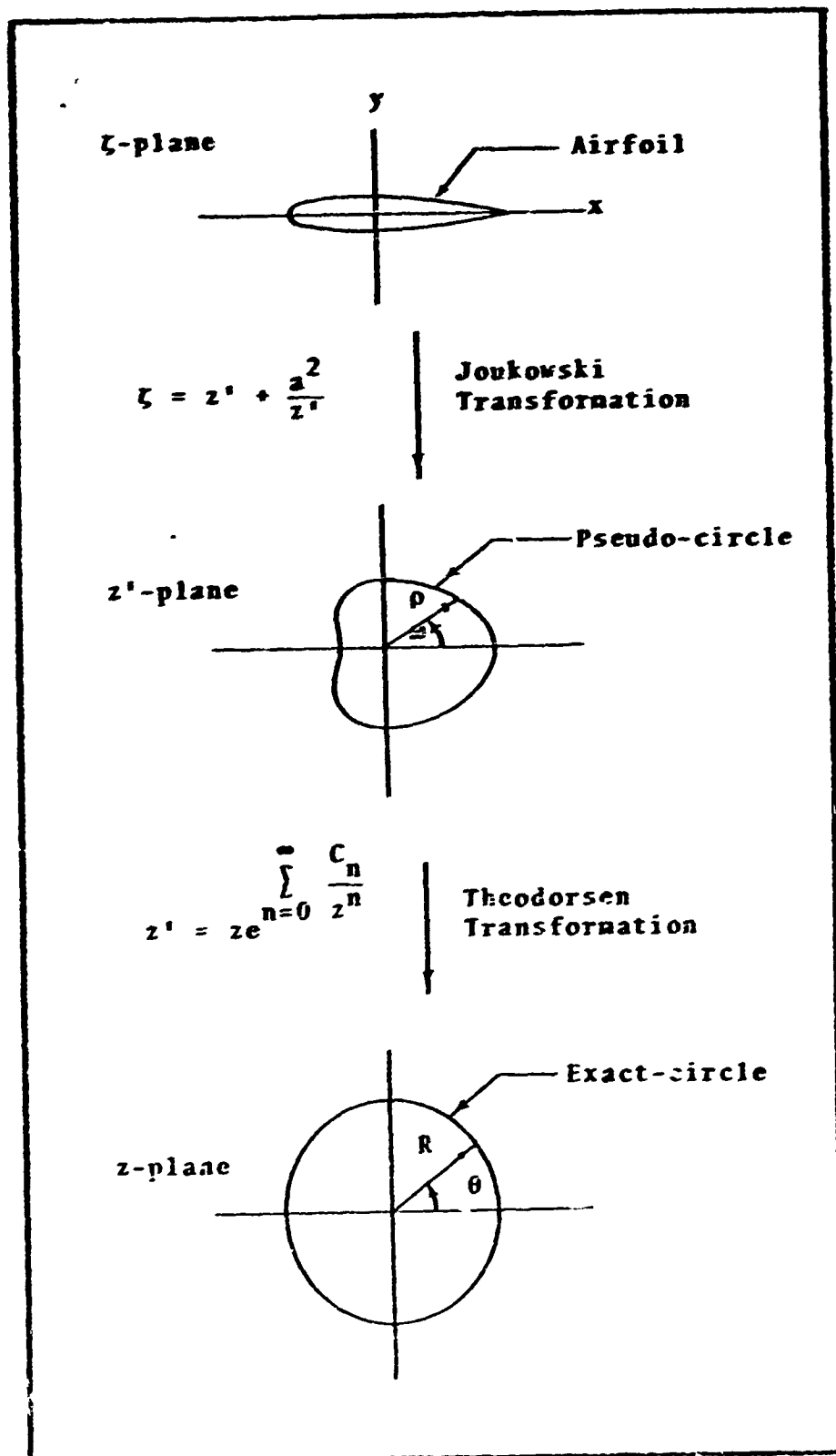


Fig. 1. Transformation Planes and Notation.

must be identical in airfoil and exact circle planes requires that  $A_0 = B_0 = 0$ . The transformation then becomes

$$z' = z e^{\sum_{n=1}^{\infty} \frac{C_n}{z^n}} = z e^{\sum_{n=1}^{\infty} \frac{A_n + iB_n}{z^n}} \quad (9)$$

Suitable means must now be found for determining the constants  $A_n$  and  $B_n$ .

The equation for the exact circle may be expressed as  $z = ae^{\phi+i\theta}$  in polar coordinates where  $\phi$  is a constant and  $R = ae^{\phi}$  is the radius vector and the angular coordinate is  $\theta$ . Eliminating the constant "a" between the polar definitions of  $z$  and  $z'$  yields

$$z' = z e^{(\psi-\phi) + i(\omega-\theta)} \quad (10)$$

Now, combining with the transformation equation

$$(\psi-\phi) + i(\omega-\theta) = \sum_{n=1}^{\infty} \frac{A_n + iB_n}{z^n} \quad (11)$$

Note that

$$z^n = (ae^{\phi+i\theta})^n = [R(\cos \theta + i \sin \theta)]^n = \frac{R^n}{\cos n\theta - i \sin n\theta} \quad (12)$$

Substituting into Eq (11)

$$(\psi - \phi) + i(\omega - \theta) = \sum_{n=1}^{\infty} \frac{A_n + iB_n}{R^n} (\cos n\theta - i \sin n\theta) \quad (13)$$

expanding

$$\begin{aligned} (\psi - \phi) + i(\omega - \theta) = \sum_{n=1}^{\infty} \left[ \frac{A_n}{R^n} \cos n\theta + \frac{B_n}{R^n} \sin n\theta \right] + \\ + i \sum_{n=1}^{\infty} \left[ \frac{B_n}{R^n} \cos n\theta - \frac{A_n}{R^n} \sin n\theta \right] \end{aligned} \quad (14)$$

and equating real and imaginary parts of Eq (14) establishes the following conjugate Fourier expansions:

$$\psi - \phi = \sum_{n=1}^{\infty} \left[ \frac{A_n}{R^n} \cos n\theta + \frac{B_n}{R^n} \sin n\theta \right] \quad (15)$$

$$\omega - \theta = \sum_{n=1}^{\infty} \left[ \frac{B_n}{R^n} \cos n\theta - \frac{A_n}{R^n} \sin n\theta \right] \quad (16)$$

The Fourier coefficients  $\frac{A_n}{R^n}$ ,  $\frac{B_n}{R^n}$ , and  $\phi$  (the constant term) of Eq (15) are given by

$$\frac{A_n}{R^n} = \frac{1}{\pi} \int_0^{2\pi} \bar{\psi}(\lambda) \cos n\lambda \, d\lambda \quad (17)$$

$$\frac{B_n}{R^n} = \frac{1}{\pi} \int_0^{2\pi} \bar{\psi}(\lambda) \sin n\lambda \, d\lambda \quad (18)$$

$$\phi = \frac{1}{2\pi} \int_0^{2\pi} \bar{\psi}(\lambda) \, d\lambda \quad (19)$$

where  $\lambda$  is an angular measure corresponding to  $\theta$  and  $\bar{\psi}(\lambda) = \psi[\omega(\lambda)]$ , since  $\psi$  is known only as a function of  $\omega$ . Therefore, a relation between  $\psi$  and  $\theta$  (or  $\lambda$ ) must be found. For any particular value of  $\theta$ , the coefficients given in Eqs (17) and (18) may be substituted into Eq (16), thereby eliminating these coefficients from that relation

$$\omega - \theta = \frac{1}{\pi} \sum_{n=1}^{\infty} \left[ \cos n\theta \int_0^{2\pi} \bar{\psi}(\lambda) \sin n\lambda d\lambda - \sin n\theta \int_0^{2\pi} \bar{\psi}(\lambda) \cos n\lambda d\lambda \right] \quad (20)$$

which reduces to

$$\omega - \theta = \frac{1}{\pi} \sum_{n=1}^{\infty} \left[ \int_0^{2\pi} \bar{\psi}(\lambda) \sin n(\lambda - \theta) d\lambda \right] = \frac{1}{\pi} \int_0^{2\pi} \bar{\psi}(\lambda) \left[ \sum_{n=1}^{\infty} \sin n(\lambda - \theta) d\lambda \right] \quad (21)$$

But,

$$\sum_{n=1}^N \sin n(\lambda - \theta) = \frac{1}{2} \cot \frac{\lambda - \theta}{2} - \frac{\cos \left[ (2N+1) \frac{\lambda - \theta}{2} \right]}{2 \sin \frac{\lambda - \theta}{2}} \quad (22)$$

so that

$$\omega - \theta = \lim_{N \rightarrow \infty} \left[ \frac{1}{2\pi} \int_0^{2\pi} \bar{\psi}(\lambda) \cot \frac{\lambda - \theta}{2} d\lambda - \frac{1}{2\pi} \int_0^{2\pi} \bar{\psi}(\lambda) \frac{\cos \left[ (2N+1) \frac{\lambda - \theta}{2} \right]}{2 \sin \frac{\lambda - \theta}{2}} d\lambda \right] \quad (24)$$

Since the second term is identically zero and the first one is unaffected in the limit,

$$\omega - \theta = \frac{1}{2\pi} \int_0^{2\pi} \bar{\psi}(\lambda) \cot \frac{\lambda - \theta}{2} d\lambda \quad (25)$$

The difference,  $(\omega - \theta)$  or  $(\omega - \lambda)$ , between angular coordinates of a point and its image in the pseudo-circle and exact circle planes is called the conformal angular distortion function, and is denoted by  $\epsilon$ , so that

$$\epsilon(\theta) = \frac{1}{2\pi} \int_0^{2\pi} \psi[\epsilon(\lambda) + \lambda] \cot \frac{\lambda - \theta}{2} d\lambda \quad (26)$$

Equation (26) is of fundamental importance in the practical application of Theodorsen's method, as it may be solved iteratively for  $\epsilon(\theta)$ , from which  $\omega(\theta)$  is obtained permitting the solution of Eq (19) for the constant  $\phi$ . Note that the relationship between polar coordinates in the pseudo-circle and exact circle planes has been obtained without having to solve for the Fourier coefficients directly.



Surface Velocity

It is shown in potential flow theory that the complex velocity potential for a circle in the  $z$ -plane immersed in steady,  $x$ -directed flow is

$$w(z) = \phi + i\psi = -V_{\infty} \left( z + \frac{R^2}{z} \right) - \frac{i\Gamma}{2\pi} \ln \frac{z}{R} \quad (27)$$

where  $V_{\infty}$  is the freestream velocity,  $R = ae^{\phi}$  is the radius of the circle, and  $\Gamma$  is the circulation. The fluid velocity in the circle plane is obtained by differentiating  $w(z)$

$$V(z) = \frac{dw}{dz} = u + iv = -V_{\infty} \left( 1 - \frac{R^2}{z^2} \right) - \frac{i\Gamma}{2\pi z} \quad (28)$$

This velocity will be zero ( $u = v = 0$ ) at stagnation points. Therefore, the locations ( $z_0$ ) of these points is given by the value for  $z$  when  $\frac{dw}{dz} = 0$ . That is,

$$z_0 = \frac{-i\Gamma \pm \sqrt{16\pi^2 R^2 V_{\infty}^2 - \Gamma^2}}{4\pi V_{\infty}} \quad (29)$$

A non-zero angle of attack  $\alpha$  may be accounted for by replacing  $z$  by  $ze^{i\alpha}$  in the real part of Eq (27). This has the effect of rotating the flow field about the circle by the angle  $\alpha$ .

$$w(z) = -V_{\infty} \left( ze^{i\alpha} + \frac{R^2}{z} e^{-i\alpha} \right) - \frac{i\Gamma}{2\pi} \ln z \quad (30)$$

and

$$V(z) = -V_{\infty} e^{i\alpha} \left( 1 - \frac{R^2}{z^2} e^{-2i\alpha} \right) - \frac{i\Gamma}{2\pi z} \quad (31)$$

The well-known Kutta-Joukowski condition requires that the trailing edge ( $\omega = \pi$ ) on an airfoil which does not have a cusped trailing edge be a stagnation point in order that infinite velocities and pressure gradients may be avoided. The circulation required to meet this condition may be found by setting  $z_0 = Re^{i(\pi+\beta)} = -Re^{i\beta}$  (where  $\beta$  is the negative of the value of  $\epsilon$  at  $\omega = \pi$ , and is called the angle of zero lift for the airfoil) and  $V(z) = 0$  in Eq (31), and solving for the corresponding  $\Gamma$ :

$$\Gamma = 4\pi R V_{\infty} \sin(\alpha + \beta) \quad (32)$$

Then

$$V(z) = \frac{dw}{dz} = -V_{\infty} e^{i\alpha} \left( 1 - \frac{R^2}{z^2} e^{-2i\alpha} \right) - i \frac{4\pi R V_{\infty} \sin(\alpha + \beta)}{2\pi z} \quad (33)$$

The velocity,  $v(z)$ , in the plane of the circle must now be converted to the velocity,  $v(\zeta)$ , at the surface of the airfoil through the use of transformation derivatives:

$$v(\zeta) = \left| \frac{dw}{d\zeta} \right| = \left| \frac{dw}{dz} \right| \left| \frac{dz}{d\zeta} \right| \left| \frac{d\zeta'}{d\zeta} \right| \quad (34)$$

and these derivatives must now be determined. Recall that  $z = Re^{i\theta}$  on the surface of the circle. Substituting this

value for  $z$  in Eq (33) gives

$$\frac{dw}{dz} = -V_0 e^{i\alpha} [1 - e^{-2i(\alpha+\theta)}] - 2iV_0 e^{-i\theta} \sin(\alpha+\beta) \quad (35)$$

which reduces to

$$\frac{dw}{dz} = -2iV_0 e^{-i\theta} [\sin(\alpha+\theta) + \sin(\alpha+\beta)] \quad (36)$$

the absolute value of which is

$$\left| \frac{dw}{dz} \right| = 2V_0 [\sin(\alpha+\theta) + \sin(\alpha+\beta)] \quad (37)$$

From the definitions of  $z$ ,  $z'$ , and  $\epsilon$

$$\frac{z'}{z} = \frac{ze^{\psi+i\omega}}{ae^{\phi+i\theta}} = e^{(\psi-\theta)+i\epsilon} \quad (38)$$

Differentiating and noting that  $\phi$  is a constant

$$\begin{aligned} \frac{dz'}{dz} &= e^{(\psi-\phi)+i\epsilon} + ze^{(\psi-\phi)+i\epsilon} \frac{d}{dz} [(\psi-\phi)+i\epsilon] = \\ &= \frac{z'}{z} [1 + z \frac{d}{dz} (\psi+i\epsilon)] \end{aligned} \quad (39)$$

But

$$\frac{1}{z} dz = \frac{1}{ae^{\phi+i\theta}} d(ae^{\phi+i\theta}) = i d\theta \quad (40)$$

Substitution into Eq (39) gives

$$\frac{dz'}{dz} = \frac{z'}{z} \left[ 1 + \frac{d(\psi + i\epsilon)}{i d\theta} \right] = \frac{z'}{z} \left( 1 - i \frac{d\psi}{d\theta} + \frac{d\epsilon}{d\theta} \right) \quad (41)$$

Further algebraic manipulation on this equation gives

$$\frac{dz'}{dz} = \frac{z'}{z} \left[ \frac{(d\theta/d\omega) + (d\epsilon/d\omega) - i (d\psi/d\omega)}{(d\theta/d\omega)} \right] \quad (42)$$

Applying the definition  $\epsilon = \omega - \theta$ , and reducing

$$\frac{dz'}{dz} = \frac{z'}{z} \left[ \frac{1 - i (d\psi/d\omega)}{1 - (d\epsilon/d\omega)} \right] \quad (43)$$

And finding the absolute value

$$\left| \frac{dz'}{dz} \right| = e^{\phi - \psi} \left[ \frac{\sqrt{1 + (d\psi/d\omega)^2}}{1 - (d\epsilon/d\omega)} \right] \quad (44)$$

Inverting

$$\left| \frac{dz}{dz'} \right| = e^{\phi - \psi} \left[ \frac{1 - (d\epsilon/d\omega)}{\sqrt{1 + (d\psi/d\omega)^2}} \right] \quad (45)$$

which is the desired derivative. Substituting the definition

$z' = ae^{\psi + i\omega}$  into the Joukowski transformation

$$\zeta = ae^{\psi + i\omega} + ae^{-\psi - i\omega} = 2a \cosh (\psi + i\omega) \quad (46)$$

Differentiating

$$\frac{d\zeta}{dz'} = 2 \sinh (\psi + i\omega) e^{-\psi - i\omega} \quad (47)$$

Expanding

$$\frac{d\zeta}{dz'} = 2e^{-\psi-i\omega} (\sinh \psi \cosh i\omega + \cosh \psi \sinh i\omega) \quad (48)$$

Noting that  $\cosh i\omega = \cos \omega$  and  $\sinh i\omega = i \sin \omega$ , this becomes

$$\frac{d\zeta}{dz'} = 2e^{-\psi-i\omega} (\sinh \psi \cos \omega + i \cosh \psi \sin \omega) \quad (49)$$

Then

$$\left| \frac{d\zeta}{dz'} \right|^2 = 4e^{-2\psi} (\sinh^2 \psi \cos^2 \omega + \cosh^2 \psi \sin^2 \omega) \quad (50)$$

which reduces to

$$\left| \frac{d\zeta}{dz'} \right|^2 = 4e^{-2\psi} (\sinh^2 \psi + \sin^2 \omega) \quad (51)$$

Taking the square root and inverting gives the final derivative

$$\left| \frac{dz'}{d\zeta} \right| = \frac{e^{\psi}}{2\sqrt{\sinh^2 \psi + \sin^2 \omega}} \quad (52)$$

The derivatives given in Eqs (37), (45), and (52) will now be substituted into Eq (34) to find the airfoil surface velocity

$$V(\zeta) = \frac{V_{\infty} e^{\phi} [\sin(\alpha+\theta) + \sin(\alpha+\beta)][1 - (d\epsilon/d\omega)]}{\sqrt{(\sinh^2 \psi + \sin^2 \omega) [1 + (d\psi/d\omega)^2]}} \quad (53)$$

This is the velocity which will then be used as an approximation for the edge velocity in the analysis of the boundary layer.

### III. Karman-Pohlhausen Method

#### Origin

General motion of a viscous fluid is described by the Navier-Stokes equations, which were derived from first principles. Schlichting (Ref 3) has shown that, if Reynolds number is large, viscosity is constant, and flow is steady and incompressible, then the equations of motion for flow over a surface may be approximated by the momentum integral equation:

$$U^2 \frac{d\delta_2}{dx} + (2\delta_2 + \delta_1) U \frac{dU}{dx} = \frac{\tau_w}{\rho} \quad (54)$$

where the boundary layer displacement and momentum thicknesses are, respectively,

$$\delta_1 = \int_0^{\infty} \left( 1 - \frac{u}{U} \right) dy \quad (55)$$

$$\delta_2 = \int_0^{\infty} \frac{u}{U} \left( 1 - \frac{u}{U} \right) dy \quad (56)$$

and where  $x$  and  $y$  are, respectively, the streamwise and cross-stream coordinates of a general point in the flow (Fig. 2), with the corresponding velocities given by  $u$  and  $v$ . Note that the boundary layer edge velocity  $U$  is a parameter common to both the potential flow and boundary layer regions.

The following analysis is due originally to Pohlhausen, but is presented in the form developed by Holstein and

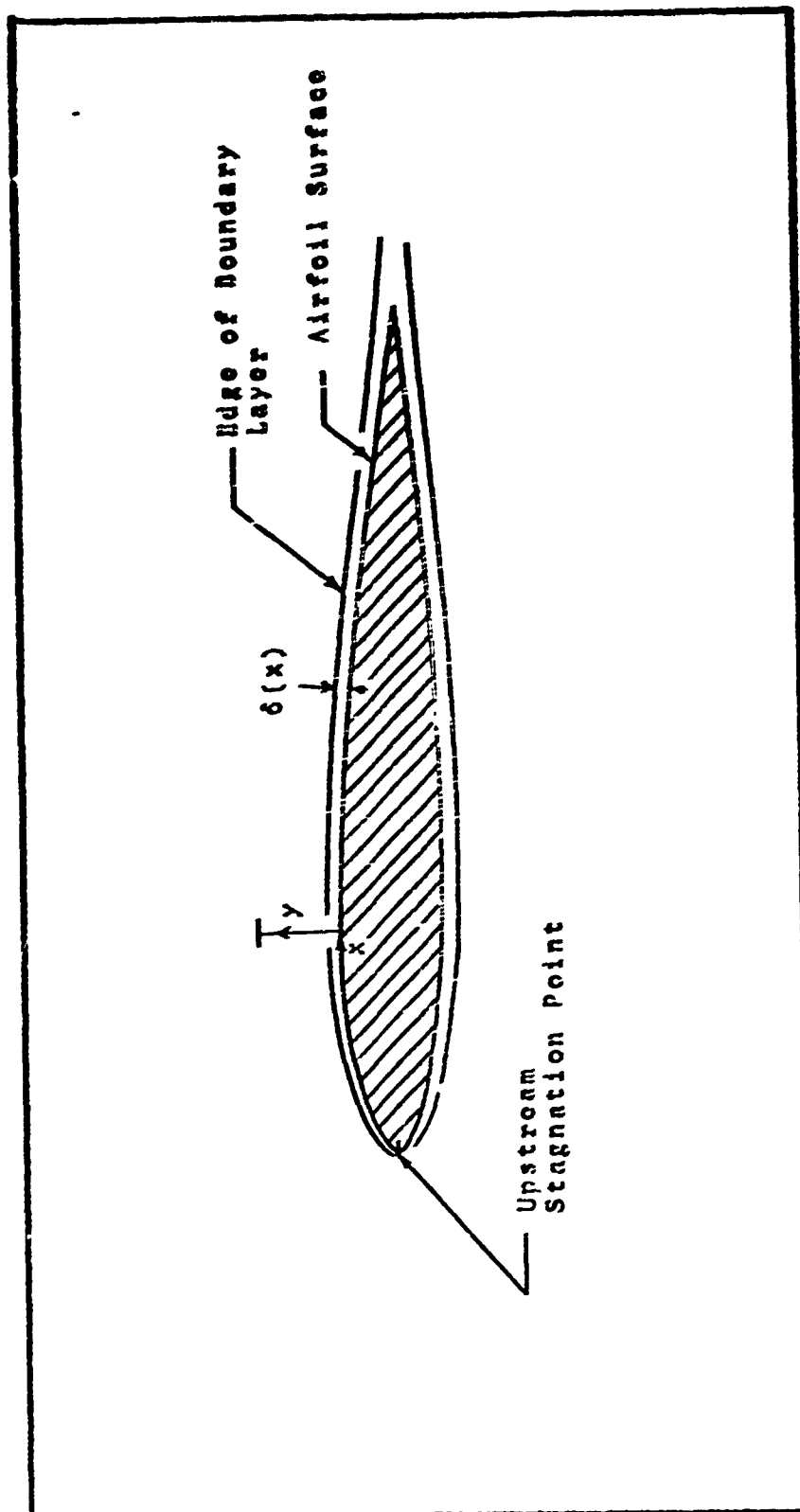


FIG. 2. Boundary Layer Coordinate System.



Bohlen, and described by Schlichting.

### Velocity Profile

A velocity profile of the following form is now assumed:

$$\frac{u}{U} = a\eta + b\eta^2 + c\eta^3 + d\eta^4 \quad (57)$$

where  $\eta = y/\delta$  and  $a$ ,  $b$ ,  $c$ , and  $d$  are coefficients to be determined.

Observations indicate that the following boundary conditions should be applied to the solution of Eq (54):

$$u = 0 \quad \text{at } y = 0 \quad (58)$$

$$v \frac{\partial^2 u}{\partial y^2} = -U \frac{dU}{dx} \quad \text{at } y = 0 \quad (59)$$

$$u = U \quad \text{at } y = \delta \quad (60)$$

$$\frac{\partial u}{\partial y} = 0 \quad \text{at } y = \delta \quad (61)$$

$$\frac{\partial^2 u}{\partial y^2} = 0 \quad \text{at } y = \delta \quad (62)$$

where  $\delta$ , called the boundary layer thickness, is the cross-stream distance from the surface at which the boundary layer meets the potential flow region.

Note that the first boundary condition, Eq (58), is identically satisfied by the assumed solution by virtue of the omission of a constant term in the polynomial. There remain, therefore, four boundary conditions to determine

a, b, c, and d. In terms of the assumed velocity profile, the second through fifth boundary conditions become, respectively,-

$$u v \left[ \frac{\partial^2}{\partial \eta^2} \left( \frac{u}{U} \right) \left( \frac{\partial \eta}{\partial y} \right)^2 \right] = -U \frac{dU}{dx} \quad \text{at } \eta = 0 \quad (63)$$

$$\frac{u}{U} = 1 \quad \text{at } \eta = 1 \quad (64)$$

$$u \left[ \frac{\partial}{\partial \eta} \left( \frac{u}{U} \frac{\partial \eta}{\partial y} \right) \right] = 0 \quad \text{at } \eta = 1 \quad (65)$$

$$u \left[ \frac{\partial^2}{\partial \eta^2} \left( \frac{u}{U} \right) \left( \frac{\partial \eta}{\partial y} \right)^2 \right] = 0 \quad \text{at } \eta = 1 \quad (66)$$

Application of these conditions to the assumed solution and defining a shape factor

$$\Lambda = \frac{\delta^2}{\nu} \frac{dU}{dx} \quad (67)$$

leads to the following expression for the velocity profile:

$$\frac{u}{U} = (2\eta - 2\eta^3 + \eta^4) + \frac{\Lambda}{6} (\eta - 3\eta^2 + 3\eta^3 - \eta^4) \quad (68)$$

By applying the physical constraints that  $\frac{\partial u}{\partial y} = 0$  at  $y = 0$  at the separation point and that  $\frac{u}{U} \leq 1$  within the boundary layer, the upper and lower physical limits on  $\Lambda$  are readily determined. These have been found to be +12 and -12, respectively.

Other Parameters

The displacement thickness, momentum thickness, and shear stress will now be found in terms of  $\Lambda$ .

Substituting the above velocity profile and the definition for  $\eta$  into the definition for displacement thickness given by Eq (55) gives

$$\frac{\delta_1}{\delta} = \int_0^1 [1 - (2\eta - 2\eta^3 + \eta^4) - \frac{\Lambda}{6} (\eta - 3\eta^2 + 3\eta^3 - \eta^4)] d\eta \quad (69)$$

And, finally,

$$\frac{\delta_1}{\delta} = \frac{3}{10} - \frac{\Lambda}{120} \quad (70)$$

Likewise,

$$\frac{\delta_2}{\delta} = \frac{37}{315} - \frac{\Lambda}{945} - \frac{\Lambda^2}{9072} \quad (71)$$

Now, the shear stress, by definition, is

$$\tau_w = \mu \left. \frac{\partial u}{\partial y} \right|_{y=0} \quad (72)$$

Evaluating the derivative and multiplying both sides by  $\frac{\delta}{\mu U}$ , gives

$$\frac{\tau_w \delta}{\mu U} = 2 + \frac{\Lambda}{6} \quad (73)$$

### Simplification of Momentum Integral Equation

The momentum integral equation can now be put into a form from which practical results may be obtained.

Multiplying both sides of Eq (54) by  $\frac{\delta_2}{v}$ , and reducing, leads to

$$\frac{\tau_w \delta_2}{\mu U} = \frac{U}{v} \delta_2 \frac{d\delta_2}{dx} + \left(2 + \frac{\delta_1}{\delta_2}\right) \frac{\delta_2^2}{v} \frac{dU}{dx} \quad (74)$$

Equations (67), (68), (70), (71), and (74), together with the known edge velocity distribution, form a solvable system. However, elimination of dependence of the other variables on  $\delta$  is desirable, since the boundary layer thickness is physically meaningless. Furthermore, the  $\frac{d\delta_2}{dx}$  quantity in Eq (74) leads to a requirement for  $\frac{d^2U}{dx^2}$  at every point on the surface. By suitable mathematical manipulation, this can be reduced to a requirement for  $\frac{d^2U}{dx^2}$  at the upstream stagnation point only. The following analysis proceeds, therefore, toward these objectives.

Introduction of several new parameters will permit simplification of the form of Eq (74). Define

$$K = \frac{\delta_2^2}{v} \frac{dU}{dx} \quad (75)$$

Then,

$$K = \left(\frac{\delta_2}{\delta}\right)^2 \frac{\delta^2}{v} \frac{dU}{dx} = \Lambda \left(\frac{\delta_2}{\delta}\right)^2 = \Lambda \left(\frac{37}{315} - \frac{\Lambda}{945} - \frac{\Lambda^2}{9072}\right)^2 \quad (76)$$

Let

$$z = \frac{\delta_2^2}{\nu} \quad (77)$$

So that

$$\frac{dz}{dx} = \frac{2}{\nu} \delta_2 \frac{d\delta_2}{dx} \quad (78)$$

Also, from Eqs (75) and (77)

$$K = z \frac{dU}{dx} \quad (79)$$

The ratio of displacement to momentum boundary layer thicknesses may be defined

$$f_1 = \frac{\delta_1}{\delta_2} \quad (80)$$

Or, using Eqs (70) and (71)

$$f_1 = \frac{\frac{\delta_1}{\delta}}{\frac{\delta_2}{\delta}} = \frac{\frac{3}{10} - \frac{\Lambda}{120}}{\frac{37}{315} - \frac{f}{945} - \frac{\Lambda^2}{9072}} \quad (81)$$

And, finally, the definition

$$f_2 = \frac{\tau_w \delta_2}{\mu U} \quad (82)$$

gives, using Eqs (71) and (73),

$$f_2 = \frac{\tau_w \delta}{\mu U} \left( \frac{\delta_2}{\delta} \right) = \left( 2 + \frac{\Lambda}{6} \right) \left( \frac{37}{315} - \frac{\Lambda}{945} - \frac{\Lambda^2}{9072} \right) \quad (83)$$

Now, if these definitions are substituted into Eq (74), the result is

$$f_2 = \frac{U}{2} \frac{dZ}{dx} + (2 + f_1)K \quad (84)$$

which may be rearranged to give

$$U \frac{dZ}{dx} = 2f_2 - (4 + 2f_1)K \quad (85)$$

The right side of Eq (85) is a function of  $\Lambda$  alone, as shown by Eqs (76), (81), and (83). Therefore, if a new parameter  $F$  is defined such that

$$F = 2f_2 - (4 + 2f_1)K \quad (86)$$

Then, it may be shown that

$$F = 2 \left( \frac{37}{315} - \frac{\Lambda}{945} - \frac{\Lambda^2}{9072} \right) \left[ 2 - \frac{116}{315} \Lambda + \left( \frac{2}{945} + \frac{1}{120} \right) \Lambda^2 + \frac{2}{9072} \Lambda^3 \right] \quad (87)$$

And Eq (85), the equation of motion, becomes

$$\frac{dZ}{dx} = \frac{F}{U} \quad (88)$$

Conditions at Stagnation Point

Enough relations now exist to permit a stepwise solution for all the boundary layer parameters, once a starting condition is known. Starting conditions, therefore, will now be determined at the upstream stagnation point.

Since the flow is brought to rest at the stagnation point,  $U_0 = 0$  (where the "o" subscript means that an associated variable is to be evaluated at stagnation point conditions). Then, from Eq (88),  $F_0$  must also be zero if  $\left( \frac{dz}{dx} \right) \Big|_0$  is to exist. Therefore,  $\Lambda_0$  must be a root of Eq (87) when  $F = 0$ . The roots of this equation are -72.2, -37.8, 7.052, 17.9, and 28.2. Because of the physical limitations on the range of  $\Lambda$ , it may be seen that

$$\Lambda_0 = 7.052 \quad (89)$$

Then from Eq (76),

$$K_0 = .0770 \quad (90)$$

And, from Eq (79),

$$Z_0 = \frac{.0770}{\left( \frac{dU}{dx} \right) \Big|_0} \quad (91)$$

which determines  $Z_0$ , since the edge velocity distribution is known from the potential flow analysis.

Now,  $\left( \frac{dz}{dx} \right) \Big|_0$  may be found by applying L'Hospital's Rule to Eq (88)

$$\left( \frac{dZ}{dx} \right) \Big|_0 = \lim_{x \rightarrow 0} \left[ \frac{(dF/dx)}{(dU/dx)} \right] = \lim_{x \rightarrow 0} \left[ \frac{(dF/dK)(dK/dx)}{(dU/dx)} \right] \quad (92)$$

But, from Eq (79),

$$\frac{dK}{dx} = \frac{dZ}{dx} \frac{dU}{dx} + Z \frac{d^2U}{dx^2} \quad (93)$$

Substituting this expression into Eq (92) and passing to the limit gives

$$\left( \frac{dZ}{dx} \right) \Big|_0 = Z_0 \left[ \frac{\left( \frac{dF}{dK} \right) \Big|_0}{1 - \left( \frac{dF}{dK} \right) \Big|_0} \right] \left[ \frac{\left( \frac{d^2U}{dx^2} \right) \Big|_0}{\left( \frac{dU}{dx} \right) \Big|_0} \right] \quad (94)$$

But, using Eqs (76) and (87),

$$\left( \frac{dF}{dK} \right) \Big|_0 = \frac{\left( \frac{dF}{d\Lambda} \right) \Big|_0}{\left( \frac{dK}{d\Lambda} \right) \Big|_0} = -5.57 \quad (95)$$

Substituting the values for  $Z_0$  and  $\left( \frac{dF}{dK} \right) \Big|_0$  given by Eqs (91) and (95), respectively, into Eq (94) provides an expression for  $\left( \frac{dZ}{dx} \right) \Big|_0$  in terms of the edge velocity distribution:

$$\left( \frac{dZ}{dx} \right) \Big|_0 = -.0652 \frac{\left( \frac{d^2U}{dx^2} \right) \Big|_0}{\left( \frac{dU}{dx} \right) \Big|_0} \quad (96)$$



Using the Method

With starting conditions known at the stagnation point, the value for  $Z$  at a distance  $\Delta x$  downstream is

$$Z_1 = Z_0 + \left( \frac{dZ}{dx} \right) \Big|_0 \Delta x \quad (97)$$

Then, from Eq (79),

$$K_1 = Z_1 \left( \frac{dU}{dx} \right) \Big|_1 \quad (98)$$

The corresponding value of  $\Lambda$ , from Eq (76) may now be used to find  $F_1$  from Eq (87). Using Eq (88),

$$\left( \frac{dZ}{dx} \right) \Big|_1 = \frac{F_1}{U_1} \quad (99)$$

so that the stepping process may be continued indefinitely, the value of  $Z$  at point "n" being

$$Z_n = Z_{n-1} + \left( \frac{dZ}{dx} \right) \Big|_{n-1} \Delta x \quad (100)$$

Knowledge of  $\Lambda_n$  permits determination of  $f_{1n}$ ,  $f_{2n}$ , and the velocity profile  $\left( \frac{u}{U} \right) \Big|_n$ , using Eqs (45), (83), and (68), respectively. Substituting  $Z_n$  into Eq (77) yields  $\delta_{2n}$ , which in turn produces  $\tau_{wn}$  from Eq (82), and, the ultimate objective,  $\delta_{1n}$  from Eq (80). This value of  $\delta_{1n}$  must be added to the original airfoil thickness to form a better

approximation of the potential flow airfoil shape to be analyzed again by Theodorsen's method.

Limitation

The Karman-Pohlhausen method of boundary layer analysis does not properly describe the flow downstream of a separation point (the point at which the shear stress at the wall vanishes).

#### IV. Computer Study

##### Purpose of Computer Study

A Fortran Extended program for the CDC-6600 computer was written as part of this study and is listed in Appendix A. It implements the theory discussed in the preceding chapters and lays a foundation for more sophisticated airfoil analysis programs. Flow parameters from this program may be compared with those from simplified airfoil theories in order to determine the validity of thin airfoil and inviscid assumptions. Some pertinent facts about the program will be discussed in this chapter.

##### Program Composition

The computer program is composed of a main program and several subprograms and functions. The main program is called MAGIC and provides the means for reading input data, controlling data flow and sequencing among subprograms, and testing for completion of the iteration on displacement thickness. One principal subprogram is THEO, which applies Theodorsen's method to the airfoil; the other is BOUND, which solves the boundary layer equations using the Karman-Pohlhausen method. Other subprograms and their purposes include: FNEVAL, which defines integrands; SIMPS, which performs integrations using Simpson's Rule; MTXEQ, which solves systems of algebraic equations; PLSQ, a polynomial least-square curve-fitting routine; ATKFN, an interpolating function; several subroutines for the CALCOMP plotter; and

numerous standard functions from the system library.

### Input

Program MAGIC requires an alphanumeric description of the airfoil (e.g., NACA 1408), the number of data points, the Cartesian coordinates of each point, a plotting index, freestream velocity, viscosity, density, and the angle of attack on the chord line. The airfoil chord line is assumed to lie on the x-axis with the trailing edge in the positive x-direction and the midchord point at the origin. Points defining the airfoil surface must begin at the trailing edge and be numbered in the counterclockwise direction. All dimensions must be referenced to chord length. The plotting index causes the airfoil and its transformations in sub-program THEO: (1) to be plotted on the same axes, (2) not to be plotted, or (3) to be plotted on separate axes, according as its value is -1, 0, or +1, respectively. The angle of attack must be given in degrees.

Additionally, accuracy requirements on various computations may be reset by modifications to the program.

### Output

Program MAGIC computes and prints Cartesian coordinates in all three planes, polar coordinates in the pseudo-circle and exact circle planes, potential flow surface velocity, coefficients for fifth-order polynomials for  $\bar{\psi}(\theta)$  and  $\psi(\omega)$ , radius of exact circle, zero-lift angle of attack, circulation, section lift, pressure coefficients, shear stress at

surface, momentum thickness, displacement thickness, shape factor, and several important quantities used in computing these. The airfoil surface in all three planes is plotted (provided that the plotting index is non-zero), as are pressure coefficient, shear stress, and displacement thickness as functions of chordwise station. Samples of output format are shown in Appendix A.

#### Limitations on Program

Although subprogram THEO gives correct results for non-zero angles of attack, subprogram BOUND does not, since the shift of upstream stagnation point with angle of attack has not been accounted for. Therefore, accurate results for the complete program may be expected only for zero angle of attack.

Values of shear stress and displacement thickness generated by subprogram BOUND downstream of the separation point become very large. These values are printed as output, but are actually limited to a reasonable maximum value before being plotted or transmitted to subprogram THEO for another iteration. In particular, the displacement thickness at the trailing edge is set to zero in order that the new airfoil shape considered by subprogram THEO will be a closed curve.

## V. Results

### Conformal Transformations

Transformations were accomplished by subprogram THEO on several airfoils, including NACA 1408 and NACA 4424. The output plot of the transformation on the NACA 4424 airfoil is presented in Fig. 3. Success of the transformation on these airfoils was measured by the accuracy of the output angle of zero lift,  $\beta$ . The values for these angles as given by Abbott and von Doenhoff (Ref 1) are presented for comparison in Table 1. Comparison data was not available for the other airfoils used.

Table 1

#### Comparison of Zero Lift Angles of Attack

<u>Airfoil</u>	<u>(Program HAGIC)</u>	<u>(Ref 5)</u>
NACA 1408	.95°	.95°
NACA 4424	3.58°	3.50°

### Potential Flow Surface Velocities

Surface velocities generated by subprogram THEO were also compared with those given by Abbott and von Doenhoff. A typical comparison is shown in Table 2. The velocities agree within 2% in most cases. Exceptions occur at points where the radius of curvature is relatively small; that is, near the leading edge. This probably reflects poor accuracies in numerical derivatives in that area.

Table 2

Comparison of Potential Flow Velocities  
for XACA 1408 Airfoil

Upper Surface			Lower Surface		
Chordwise Station (percent chord)	$V/V_\infty$ (Program MAGIC)	$V/V_\infty$ (Ref 1)	Chordwise Station (Percent chord)	$V/V_\infty$ (Program MAGIC)	$V/V_\infty$ (Ref 1)
0	0	0	0	0	0
1.189	.780	1.061	1.311	.829	1.039
2.413	1.067	1.121	2.582	1.079	1.039
4.896	1.135	1.151	5.104	1.121	1.105
7.386	1.142	1.161	7.614	1.112	1.105
9.883	1.145	1.161	10.117	1.102	1.099
14.889	1.153	1.164	15.111	1.096	1.092
19.904	1.152	1.162	20.096	1.085	1.082
24.926	1.148	1.157	25.074	1.075	1.071
29.950	1.139	1.149	30.050	1.065	1.063
40.000	1.126	1.131	40.000	1.054	1.047
50.020	1.107	1.110	49.980	1.038	1.034
60.034	1.087	1.089	59.966	1.023	1.019
70.041	1.067	1.070	69.959	1.012	1.008
80.039	1.042	1.043	79.961	.998	.991
90.027	1.014	1.003	89.973	.982	.965
95.016	.966	.983	94.984	.953	.955
100.000	0	0	100.000	0	0

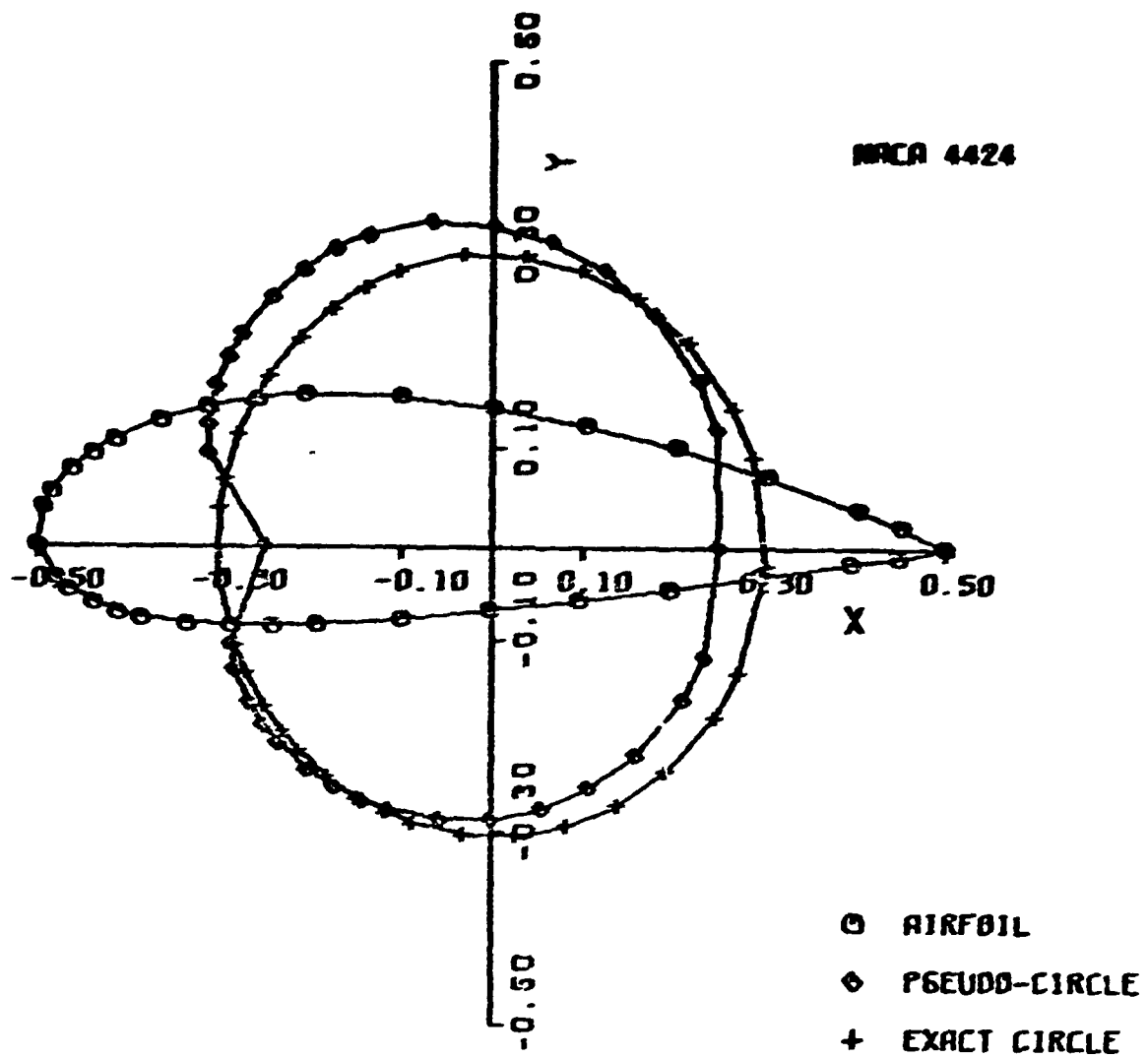


Fig. 3. Transformation of NACA 4424 Airfoil.



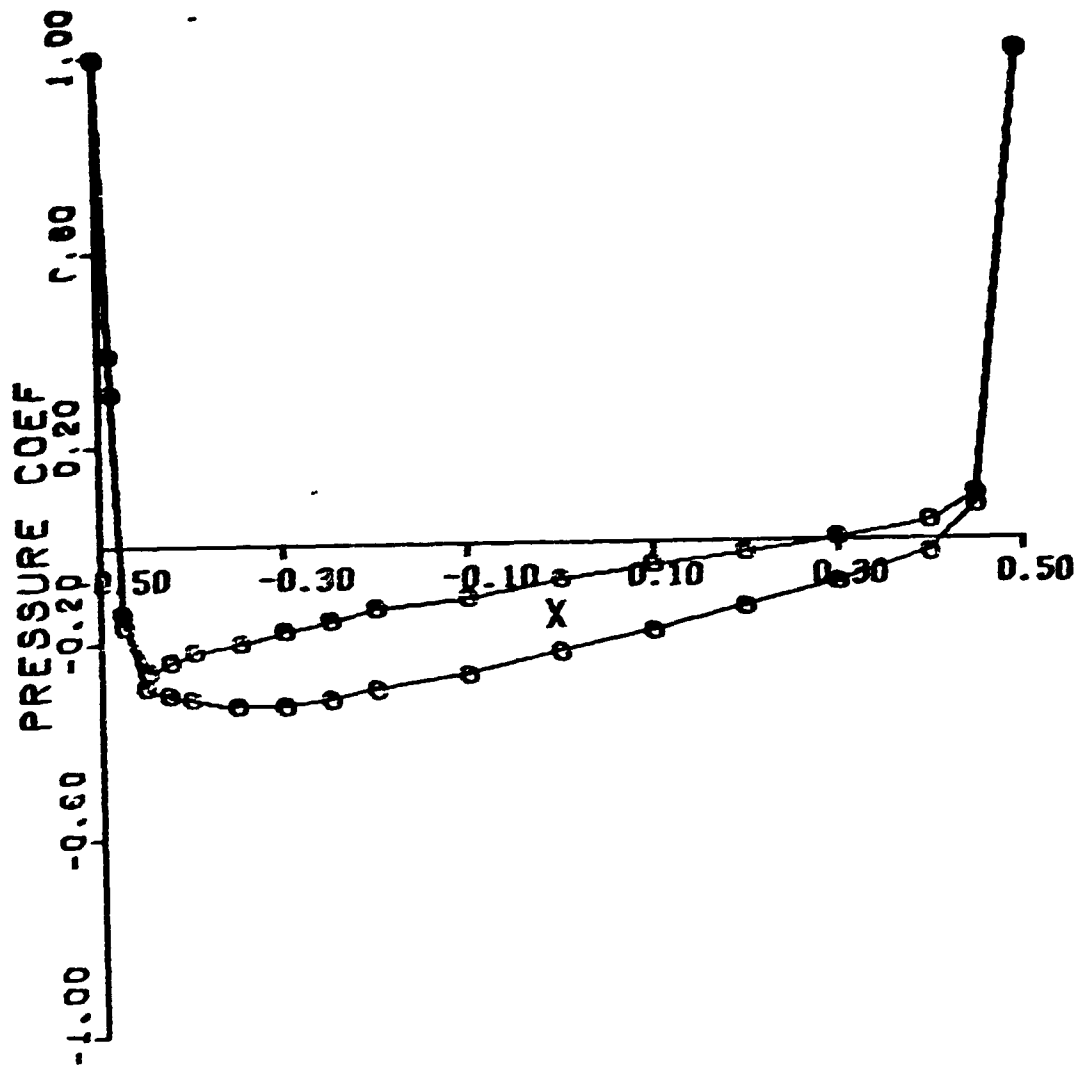


Fig. 4. Pressure Distribution on NACA 1408 Airfoil.

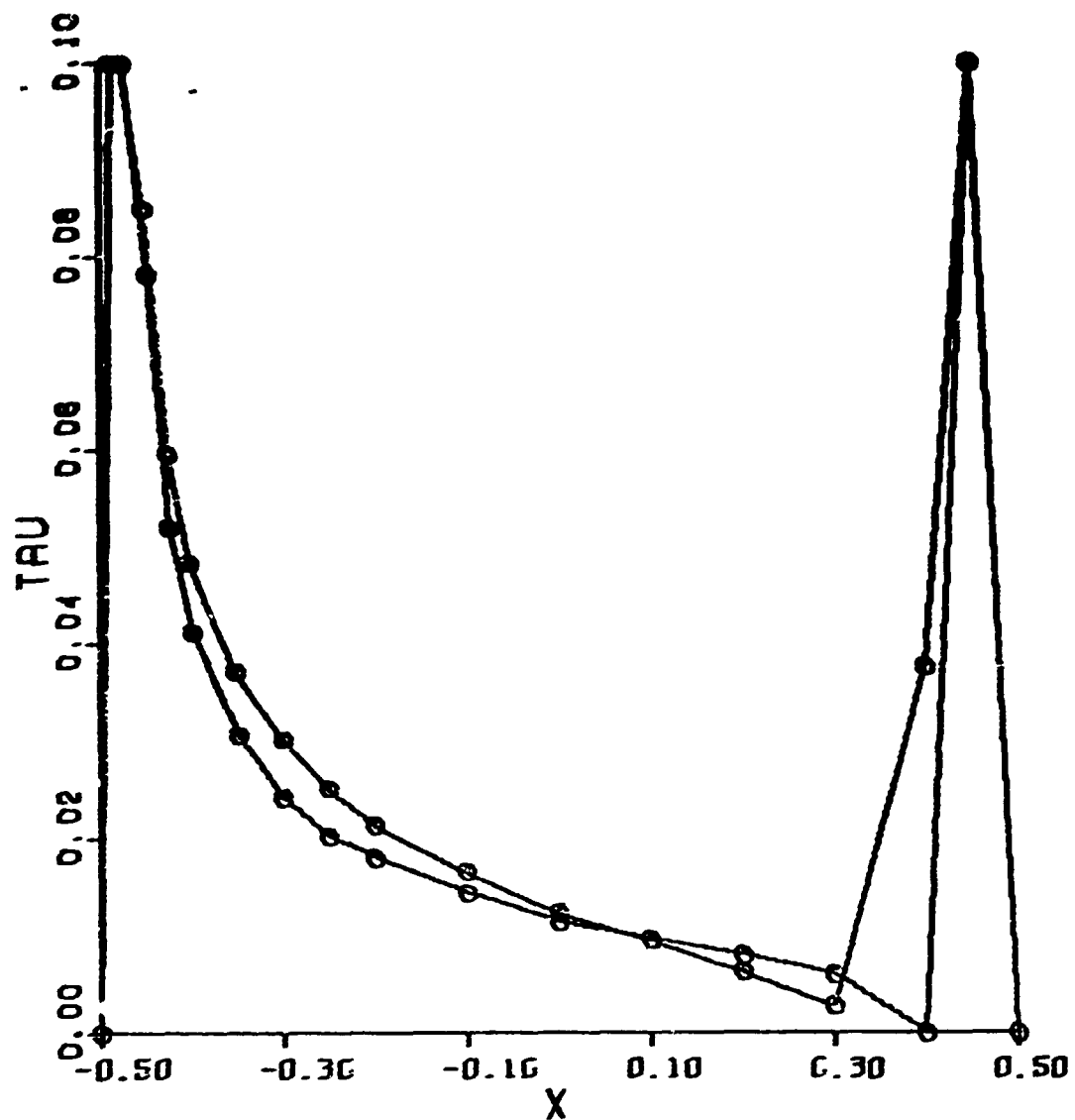


Fig. 5. Shear Stress on NACA 1408 Airfoil.

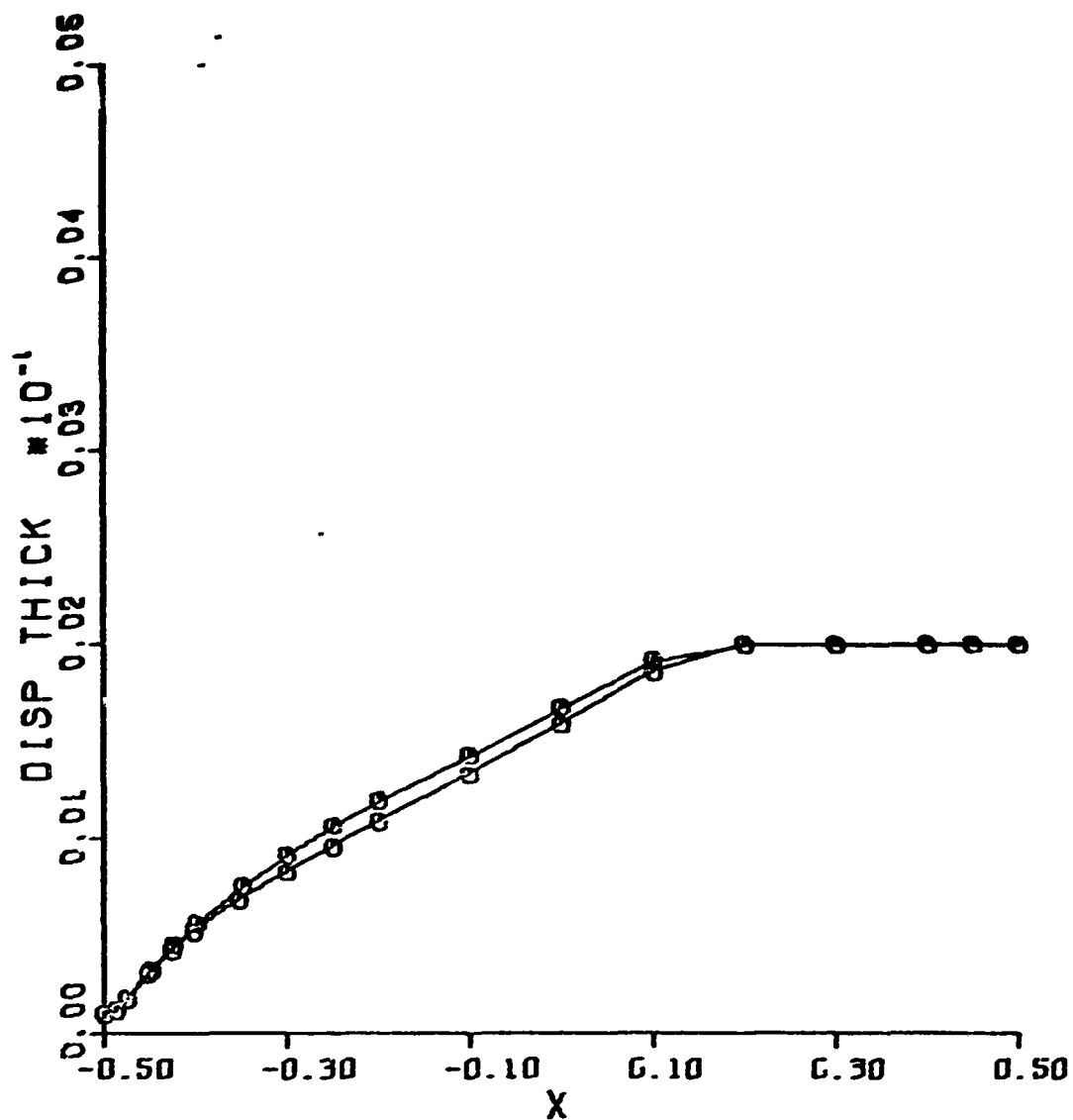


Fig. 6. Boundary Layer Displacement Thickness on NACA 1408 Airfoil.

### Boundary Layer Parameters

Pressure coefficients, shear stress, and boundary layer displacement thickness distributions are qualitatively correct (Figs. 4, 5, and 6) upstream of the separation point. As a quantitative check, the separation point for uniform flow around a circle was computed. Subprogram BOUND found this point to be at  $105^\circ$  from the upstream stagnation point. This agrees well with values from  $104.5^\circ$  to  $108.8^\circ$  determined by various investigators, as cited by Schlichting.

### Running Time and Core Memory Required

Computer time required for program MAGIC is a function of airfoil shape, number of points, and accuracy required. The NACA 1408 airfoil, with 34 points defined, required approximately 50 seconds of CDC-6600 central processor time and two iterations to obtain a displacement thickness accuracy of .1% of chord length.

Approximately 40,000 octal words of core memory were required.

## VI. Conclusions and Recommendations

### Conclusions

Based upon the results shown in the preceding chapter, the following conclusions were drawn from this study:

1. Theodorsen's method computes values of zero lift angle of attack and potential flow surface velocities very accurately.

2. The Karman-Pohlhausen method of solving the boundary layer equations yields good results upstream of the separation point. No useful information is obtained from these equations downstream of the separation point. Knowledge of the shape factor permits determination of the coefficients in the assumed velocity profile at any point along the surface.

3. Program MAGIC is a practical means of analyzing incompressible flow about an airfoil, without resort to small perturbation or inviscid assumptions. Core memory and central processor requirements are very reasonable for an analysis of this magnitude. Input data requirements are minimal.

### Recommendations

The following recommendations are made for future studies in extension of this one:

1. Program BOUND could be modified to permit boundary layer computations when angle of attack is not zero.

2. Integration of pressure distribution and shear stress would provide drag, moment, and center of pressure information.

3. According to Giesing (Ref 2), Theodorsen's method can be extended to linear arrangements of identical airfoils. Program MAGIC, so extended, could be of considerable value in cascade theory.

4. Theodorsen states that accounting for leading edge and trailing edge radii in locating the coordinate system origin improves the rate of convergence of the iteration on  $\epsilon$ . Inclusion of this correction might result in some saving in computer time.

5. Numerical derivatives of a higher order of accuracy near the leading edge would probably improve velocities computed in that region.

6. The inverse problem (see Ref 4) could be programmed. That is, given a desired pressure distribution, the required airfoil shape could be determined.

7. A more graphic means of input and output could be obtained by adapting the program to the cathode ray tube display terminal.

Bibliography

1. Abbott, Ira H. and Albert E. von Doenhoff. Theory of Wing Sections. New York: McGraw-Hill Book Co., 1949.
2. Giesing, Joseph P. Potential Flow About Two-Dimensional Airfoils. Report No. LB31946. McDonnell-Douglas Aircraft Company, 1 December 1965 (Revised 10 May 1968).
3. Schlichting, H. Boundary Layer Theory (Sixth Edition). New York: McGraw-Hill Book Co., 1968.
4. Theodorsen, T. and I. E. Garrick. General Potential Theory of Arbitrary Wing Sections. NACA Report No. 452. Washington: National Advisory Committee for Aeronautics, 1933.

Appendix A

Computer Program and Sample Output Format

Reproduced from  
best available copy.



\*\*\*\*\*  
 \*\*\*\*\*  
 \*\*\*\*\*

PROGRAM MAGIC (INPUT, OUTPUT, STATEMENT, TABLE, OUTPUT, PLOT)

MAGIC IS A GENERALIZED PROGRAM FOR ANALYSIS OF STEADY, VISCOUS, INCOMPRESSIBLE, TWO-DIMENSIONAL FLOW AROUND AN AIRFOIL OF ARBITRARY SHAPE. IT UTILIZES THE CHARACTERISTICS METHOD AND THE KERN-FORMULA FOR THE CALCULATION OF THE SURFACES. OUTPUTS ARE DESCRIBED IN THE FOLLOWING TWO AND FOUR.

MAGIC PERFORMS THE FOLLOWING INPUTS (FOR INPUT):

- 1. DESIGNATION OF AIRFOIL (AIR)
- 2. NUMBER OF POINTS (N)
- 3. X AND Y FOR EACH POINT (X(I), Y(I))
- 4. PLACING TWO POINTS (X1, Y1, X2, Y2)
- 5. ANGLE OF ATTACK (ALPHA)
- 6. REYNOLDS NUMBER (REYN)
- 7. VISCOSITY, ABSOLUTE VISCOSITY, SPECIFIC HEAT (MU, C, K)

THE NUMBER OF POINTS IS LIMITED TO 47. SEE SUBROUTINE TWO FOR ADDITIONAL INPUT DATA REQUISITES.

MAGIC PROVIDES APPROXIMATELY 40,000 POINTS OF DATA. THE NUMBER OF POINTS, AND ACCURACY OF RESULTS, IS A FUNCTION OF AIRFOIL SHAPE, NUMBER OF POINTS, AND ACCURACY REQUIRED.

DESCRIPTION OF MAGICAL OUTPUT VARIABLES:

1. AERODYNAMIC HIGH-TO-LOW ORDER COEFFICIENTS OF DRAG (CD), LIFT (CL), MOMENT (CM).

2. AERODYNAMIC HIGH-TO-LOW ORDER COEFFICIENTS OF DRAG (CD), LIFT (CL), MOMENT (CM).

3. CD IS DISPLACEMENT MOMENTUM.

4. CD IS MOMENTUM INTEGRAL.

5. CD IS SHEAR STRESS AT THE AIRFOIL SURFACE.

6. CM IS THE SHAP FACTOR.

7. (X, Y), (X, Y), AND (X, Y) ARE CARTESIAN COORDINATES IN THE THREE TRANSFORMATION PLANE.

8. (X, Y), (X, Y), AND (X, Y) ARE POLAR COORDINATES IN THE POLAR-CIRCLE PLANE.

9. CD IS THE MAGNIFICATION FACTOR IN THE POLAR-CIRCLE PLANE.

10. CD IS THE CENTRAL MAGNIFICATION FACTOR IN THE POLAR-CIRCLE PLANE.

11. CD IS THE SURFACE VELOCITY/PERCENTAGE VELOCITY RATIO.

12. CD IS THE PRESSURE COEFFICIENT.

13. CD IS (OMEGA-THETA).

14. ALPHA IS THE ANGLE OF ATTACK.





0202

CEC 0030 07A W3-C-101A CPTA 11/06/91 16:29:59.

CONFIDENTIAL T-147 PAGE 2

ALL INFORMATION CONTAINED HEREIN IS UNCLASSIFIED

3  
5  
7  
9  
11  
13  
15  
17  
19  
21  
23  
25  
27  
29  
31  
33  
35  
37  
39  
41  
43  
45  
47  
49  
51  
53  
55  
57  
59  
61  
63  
65  
67  
69  
71  
73  
75  
77  
79  
81  
83  
85  
87  
89  
91  
93  
95  
97  
99  
101  
103  
105  
107  
109  
111  
113  
115  
117  
119  
121  
123  
125  
127  
129  
131  
133  
135  
137  
139  
141  
143  
145  
147  
149  
151  
153  
155  
157  
159  
161  
163  
165  
167  
169  
171  
173  
175  
177  
179  
181  
183  
185  
187  
189  
191  
193  
195  
197  
199  
201  
203  
205  
207  
209  
211  
213  
215  
217  
219  
221  
223  
225  
227  
229  
231  
233  
235  
237  
239  
241  
243  
245  
247  
249  
251  
253  
255  
257  
259  
261  
263  
265  
267  
269  
271  
273  
275  
277  
279  
281  
283  
285  
287  
289  
291  
293  
295  
297  
299  
301  
303  
305  
307  
309  
311  
313  
315  
317  
319  
321  
323  
325  
327  
329  
331  
333  
335  
337  
339  
341  
343  
345  
347  
349  
351  
353  
355  
357  
359  
361  
363  
365  
367  
369  
371  
373  
375  
377  
379  
381  
383  
385  
387  
389  
391  
393  
395  
397  
399  
401  
403  
405  
407  
409  
411  
413  
415  
417  
419  
421  
423  
425  
427  
429  
431  
433  
435  
437  
439  
441  
443  
445  
447  
449  
451  
453  
455  
457  
459  
461  
463  
465  
467  
469  
471  
473  
475  
477  
479  
481  
483  
485  
487  
489  
491  
493  
495  
497  
499  
501  
503  
505  
507  
509  
511  
513  
515  
517  
519  
521  
523  
525  
527  
529  
531  
533  
535  
537  
539  
541  
543  
545  
547  
549  
551  
553  
555  
557  
559  
561  
563  
565  
567  
569  
571  
573  
575  
577  
579  
581  
583  
585  
587  
589  
591  
593  
595  
597  
599  
601  
603  
605  
607  
609  
611  
613  
615  
617  
619  
621  
623  
625  
627  
629  
631  
633  
635  
637  
639  
641  
643  
645  
647  
649  
651  
653  
655  
657  
659  
661  
663  
665  
667  
669  
671  
673  
675  
677  
679  
681  
683  
685  
687  
689  
691  
693  
695  
697  
699  
701  
703  
705  
707  
709  
711  
713  
715  
717  
719  
721  
723  
725  
727  
729  
731  
733  
735  
737  
739  
741  
743  
745  
747  
749  
751  
753  
755  
757  
759  
761  
763  
765  
767  
769  
771  
773  
775  
777  
779  
781  
783  
785  
787  
789  
791  
793  
795  
797  
799  
801  
803  
805  
807  
809  
811  
813  
815  
817  
819  
821  
823  
825  
827  
829  
831  
833  
835  
837  
839  
841  
843  
845  
847  
849  
851  
853  
855  
857  
859  
861  
863  
865  
867  
869  
871  
873  
875  
877  
879  
881  
883  
885  
887  
889  
891  
893  
895  
897  
899  
901  
903  
905  
907  
909  
911  
913  
915  
917  
919  
921  
923  
925  
927  
929  
931  
933  
935  
937  
939  
941  
943  
945  
947  
949  
951  
953  
955  
957  
959  
961  
963  
965  
967  
969  
971  
973  
975  
977  
979  
981  
983  
985  
987  
989  
991  
993  
995  
997  
999  
1001  
1003  
1005  
1007  
1009  
1011  
1013  
1015  
1017  
1019  
1021  
1023  
1025  
1027  
1029  
1031  
1033  
1035  
1037  
1039  
1041  
1043  
1045  
1047  
1049  
1051  
1053  
1055  
1057  
1059  
1061  
1063  
1065  
1067  
1069  
1071  
1073  
1075  
1077  
1079  
1081  
1083  
1085  
1087  
1089  
1091  
1093  
1095  
1097  
1099  
1101  
1103  
1105  
1107  
1109  
1111  
1113  
1115  
1117  
1119  
1121  
1123  
1125  
1127  
1129  
1131  
1133  
1135  
1137  
1139  
1141  
1143  
1145  
1147  
1149  
1151  
1153  
1155  
1157  
1159  
1161  
1163  
1165  
1167  
1169  
1171  
1173  
1175  
1177  
1179  
1181  
1183  
1185  
1187  
1189  
1191  
1193  
1195  
1197  
1199  
1201  
1203  
1205  
1207  
1209  
1211  
1213  
1215  
1217  
1219  
1221  
1223  
1225  
1227  
1229  
1231  
1233  
1235  
1237  
1239  
1241  
1243  
1245  
1247  
1249  
1251  
1253  
1255  
1257  
1259  
1261  
1263  
1265  
1267  
1269  
1271  
1273  
1275  
1277  
1279  
1281  
1283  
1285  
1287  
1289  
1291  
1293  
1295  
1297  
1299  
1301  
1303  
1305  
1307  
1309  
1311  
1313  
1315  
1317  
1319  
1321  
1323  
1325  
1327  
1329  
1331  
1333  
1335  
1337  
1339  
1341  
1343  
1345  
1347  
1349  
1351  
1353  
1355  
1357  
1359  
1361  
1363  
1365  
1367  
1369  
1371  
1373  
1375  
1377  
1379  
1381  
1383  
1385  
1387  
1389  
1391  
1393  
1395  
1397  
1399  
1401  
1403  
1405  
1407  
1409  
1411  
1413  
1415  
1417  
1419  
1421  
1423  
1425  
1427  
1429  
1431  
1433  
1435  
1437  
1439  
1441  
1443  
1445  
1447  
1449  
1451  
1453  
1455  
1457  
1459  
1461  
1463  
1465  
1467  
1469  
1471  
1473  
1475  
1477  
1479  
1481  
1483  
1485  
1487  
1489  
1491  
1493  
1495  
1497  
1499  
1501  
1503  
1505  
1507  
1509  
1511  
1513  
1515  
1517  
1519  
1521  
1523  
1525  
1527  
1529  
1531  
1533  
1535  
1537  
1539  
1541  
1543  
1545  
1547  
1549  
15

THE FOLLOWING TABLE

11-20-66 11:58 AM

1944

11-11-68

**SECRET**

7-4-64-61

100

...

**SECRET**

With the "Chlorine" Method, the chlorine is added to the water in the form of a gas. The chlorine gas is added to the water in the form of a gas. The chlorine gas is added to the water in the form of a gas.

**THE UNIVERSITY OF CHICAGO**

SECRETARY OF THE ARMY  
WASHINGTON, D. C. 20315-5000

**00000000000000000000000000000000**

10-10-68

(continued)

THE UNIVERSITY OF CHICAGO

[illegible]

10/10/2010 10:10:10

100-443887-100

• 1997 •

—

1000

1000

09-08-2017

(000009) / ((112A(11)A(6)A(11)A(7)=8V

**ALL INFORMATION CONTAINED HEREIN IS UNCLASSIFIED**

THE UNIVERSITY OF CHICAGO

**JJ-06897**

**00000000000000000000**

010 44 312

\_\_\_\_\_



Page	Page	Page
100	101	102
103	104	105
106	107	108
109	110	111
112	113	114
115	116	117
118	119	120
121	122	123
124	125	126
127	128	129
130	131	132
133	134	135
136	137	138
139	140	141
142	143	144
145	146	147
148	149	150
151	152	153
154	155	156
157	158	159
160	161	162
163	164	165
166	167	168
169	170	171
172	173	174
175	176	177
178	179	180
181	182	183
184	185	186
187	188	189
190	191	192
193	194	195
196	197	198
199	200	201
202	203	204
205	206	207
208	209	210
211	212	213
214	215	216
217	218	219
220	221	222
223	224	225
226	227	228
229	230	231
232	233	234
235	236	237
238	239	240
241	242	243
244	245	246
247	248	249
250	251	252
253	254	255
256	257	258
259	260	261
262	263	264
265	266	267
268	269	270
271	272	273
274	275	276
277	278	279
280	281	282
283	284	285
286	287	288
289	290	291
292	293	294
295	296	297
298	299	300
301	302	303
304	305	306
307	308	309
310	311	312
313	314	315
316	317	318
319	320	321
322	323	324
325	326	327
328	329	330
331	332	333
334	335	336
337	338	339
340	341	342
343	344	345
346	347	348
349	350	351
352	353	354
355	356	357
358	359	360
361	362	363
364	365	366
367	368	369
370	371	372
373	374	375
376	377	378
379	380	381
382	383	384
385	386	387
388	389	390
391	392	393
394	395	396
397	398	399
400	401	402
403	404	405
406	407	408
409	410	411
412	413	414
415	416	417
418	419	420
421	422	423
424	425	426
427	428	429
430	431	432
433	434	435
436	437	438
439	440	441
442	443	444
445	446	447
448	449	450
451	452	453
454	455	456
4		

- 52 -







[illegible]





[illegible]

**Page**

[illegible]

**278 CONTINUED**

SECRET

```
X(1:3)=0.5
Y(1:2)=.2
TAN(1:3)=.
TAN(1:2)=.2
CALL PLOTIC.
CALL PLOTIC.
CALL PLOTIC.
CALL PLOTIC.
CALL PLOTIC.
```

ASSASSINATE ANOTHER DISJUNCT

```
V(M01)=.5  
V(M02)=.2  
V(L1M01)=0.  
V(L1M02)=.001  
CALL PLOT(10.,-10.-3)  
CALL PLT(10.,-10.-7)  
CALL ATX(10.,-10.-9)  
CALL ATY(10.,-10.-5).2)  
CALL LINE(VFL,N,1,1)  
CALL PLOT(10.,0.-3)  
1027 CONTINUE
```

Reproduced from  
best available copy.





SUBROUTINE MATHN YRAC

CALL SYSTEM (207,10 )

STOP

1000 FORMAT(1H=12.00, 12H=12.00 ARE INCOMPAT FOR SUPERUTINE MATHN)

1001 FORMAT (1H=12.00 ARE INCOMPAT FOR SUPERUTINE MATHN)

END

MTX0011  
MTX0012  
MTX0013  
MTX0014  
MTX0015

Reproduced from  
best available copy. (C)







SUBROUTINE PLSO(X,Y,N,K,C,LIST,EMX,EMPS,FMFO)

PLSO POLYNOMIAL LEAST SQUARE CURVE FIT

PLSO WILL FIT A GIVEN SET OF DATA TO A  
POLYNOMIAL OF DEGREE K OF THE FORM...

$$Y = C(1) + C(2)X + C(3)X^2 + \dots + C(K+1)X^K$$

PLSO THEN COMPUTES THE MAXIMUM ERROR AND ROOT  
MEAN SQUARE ERROR OBTAINED BY USING THE C  
COEFFICIENTS TO COMPUTE Y FROM X

USING...

FUNCTION Y(N), Y(N), C(L)

WHERE L IS K+1

CALL PLSO(X,Y,N,K,C,LIST,EMX,EMPS,FMFO)

WHERE,

X IS THE ARRAY OF N INDEPENDENT VARIABLES

Y IS THE ARRAY OF N DEPENDENT VARIABLES

N IS THE NUMBER OF INDEPENDENT  
VARIABLES

K IS THE DEGREE OF THE LEAST SQUARES POLYNOMIAL

C IS THE ARRAY OF THE COEFFICIENTS, HIGH ORDER  
TO LOW ORDER, OF THE LEAST SQUARES POLYNOMIAL

LIST = 1 SURVEYS THE ERROR ANALYSIS OUTPUT  
= 2 GIVES THE ERROR ANALYSIS OUTPUT

EMX IS THE MAXIMUM ABSOLUTE ERROR OBTAINED  
BY USING THE COMPUTED C COEFFICIENTS TO  
APPROXIMATE THE DEPENDENT VARIABLE

EMPS IS THE ROOT MEAN SQUARE ERROR OBTAINED  
BY USING THE COMPUTED C COEFFICIENTS TO  
APPROXIMATE THE DEPENDENT VARIABLE

FMFO IS THE MAXIMUM DEVIATION FROM UNITY  
IN THE LINEAR SYSTEM CHECK SOLUTION

PLSO CALLS SUBROUTINE PLSO

PLSO USES 1319 CELLS OF PLANK COMMON

COMMON /PLX/OT(664), OF, OIF, I, J, JC, JM,

PLSC0001  
PLSC0002  
PLSC0003  
PLSC0004  
PLSC0005  
PLSC0006  
PLSC0007  
PLSC0008  
PLSC0009  
PLSC0010  
PLSC0011  
PLSC0012  
PLSC0013  
PLSC0014  
PLSC0015  
PLSC0016  
PLSC0017  
PLSC0018  
PLSC0019  
PLSC0020  
PLSC0021  
PLSC0022  
PLSC0023  
PLSC0024  
PLSC0025  
PLSC0026  
PLSC0027  
PLSC0028  
PLSC0029  
PLSC0030  
PLSC0031  
PLSC0032  
PLSC0033  
PLSC0034  
PLSC0035  
PLSC0036  
PLSC0037  
PLSC0038  
PLSC0039  
PLSC0040  
PLSC0041  
PLSC0042  
PLSC0043  
PLSC0044  
PLSC0045  
PLSC0046  
PLSC0047  
PLSC0048  
PLSC0049  
PLSC0050  
PLSC0051  
PLSC0052  
PLSC0053  
PLSC0054  
PLSC0055

165







**PAGE 1**

**16.29.88.**

**CDC 6600 FTM V3.0-201A OPTm2**

**SLAPCUTIAE SIMPS**      **TRACF**

[illegible]

Reproduced from  
best available copy.

4	1	2	3	4	5	6	7	8	9	10	11	12	13	14	15	16	17	18	19	20	21	22	23	24	25	26	27	28	29	30	31	32	33	34	35	36	37	38	39	40	41	42	43	44	45	46	47	48	49	50	51	52	53	54	55	56	57	58	59	60	61	62	63	64	65	66	67	68	69	70	71	72	73	74	75	76	77	78	79	80	81	82	83	84	85	86	87	88	89	90	91	92	93	94	95	96	97	98	99	100
1	2	3	4	5	6	7	8	9	10	11	12	13	14	15	16	17	18	19	20	21	22	23	24	25	26	27	28	29	30	31	32	33	34	35	36	37	38	39	40	41	42	43	44	45	46	47	48	49	50	51	52	53	54	55	56	57	58	59	60	61	62	63	64	65	66	67	68	69	70	71	72	73	74	75	76	77	78	79	80	81	82	83	84	85	86	87	88	89	90	91	92	93	94	95	96	97	98	99	100	

23030330





Reproduced from  
best available copy.

24 --2011400 --21400-01  
25 --17600-00 --21400-01  
26 --1584000 --25765-01  
27 --1182000 --26665-01  
28 --1102000 --26665-01  
29 --77490-01 --26675-01  
30 --46500-01 --27475-01  
31 --27950-01 --28065-01  
32 --44705-02 --28615-01  
33 --39715-01 --28615-01  
34 --91920-01 --28615-01  
35 --10000-01 --28615-01

C  
--22005-03 --21765-07  
--13500-02 --21765-07  
--18600-01 --18715-01  
--22000-01 --18715-01  
--55000-01 --28615-01  
--55000-01 --28615-01

PMR .65700-01 EX .21000-01 ALGMA 1.0  
CIRCULATION .50000-01 LIFE .31770-01  
MFR .05000-01 MFR



Reproduced from  
best available copy.

*[The page contains two large rectangular areas filled with dense, illegible black marks, likely representing redacted information or extremely poor quality scan artifacts.]*





Vita

Ellie B. Underwood, Jr., was born on 27 January 1939 in Beeville, Texas. He was graduated in June 1956 from Ballinger High School, Ballinger, Texas. In June 1961, he was awarded a Bachelor of Science degree in Aerospace Engineering from the University of Texas, Austin, Texas, and was commissioned in the United States Air Force at the same time. In June 1960, he was assigned to the Air Force Institute of Technology, Wright-Patterson Air Force Base, Ohio.

Permanent Address: P.O. Box 592

Ballinger, Texas 76821

This thesis was typed by Jane Manemann.